Nanoscale

COMMUNICATION

View Article Online
View Journal | View Issue

Cite this: *Nanoscale*, 2015, **7**, 1601

Received 17th September 2014,
Accepted 7th December 2014

DOI: 10.1039/c4nr05410e

www.rsc.org/nanoscale

Broadband infrared photoluminescence in silicon nanowires with high density stacking faults†

Yang Li,[a] Zhihong Liu,[b] Xiaoxiang Lu,[a] Zhihua Su,[a] Yanan Wang,[a] Rui Liu,[c] Dunwei Wang,[c] Jie Jian,[d] Joon Hwan Lee,[d] Haiyan Wang,[d] Qingkai Yu*[b] and Jiming Bao*[a]

Making silicon an efficient light-emitting material is an important goal of silicon photonics. Here we report the observation of broadband sub-bandgap photoluminescence in silicon nanowires with a high density of stacking faults. The photoluminescence becomes stronger and exhibits a blue shift under higher laser powers. The super-linear dependence on excitation intensity indicates a strong competition between radiative and defect-related non-radiative channels, and the spectral blue shift is ascribed to the band filling effect in the heterostructures of wurtzite silicon and cubic silicon created by stacking faults.

Silicon is an indirect bandgap semiconductor with a weak optical response. There have been enormous efforts in making silicon optically more active either above or below its bandgap despite many scientific and technological challenges.[1] Creating nanocrystals of silicon is probably the most successful approach toward engineering silicon for visible light emission above the bandgap.[1–4] The emission spectrum can be further tuned by varying the size of nanocrystals. In contrast, it is more difficult to modify silicon for sub-bandgap infrared light emission, especially at room temperature. One approach is to incorporate impurity elements into silicon, such as Er or carbon to create optically active extrinsic defects.[5–7] Another approach is to make use of intrinsic defects of silicon, such as point defects, rod-like defects, dislocations or line defects.[5,8–10] However, unlike silicon nanocrystals, emission spectra from these impurities or defects exhibit characteristics of these defects, and can be hardly tuned. Furthermore, most of these infrared emissions are strong only at low temperature, and become quenched at room temperature.

In this letter, we report the observation of broadband infrared photoluminescence at room-temperature from a new type of intrinsic defects: stacking fault, which were created during chemical synthesis of Si nanowires. The emission covers a wide spectrum from 1.2 to 1.5 μm, which is very different from those observed in dislocations or Si/SiO_2 interfaces.[11–13] The photoluminescence shows a nonlinear dependence on the excitation laser power, which becomes much stronger and blue-shifted at higher laser excitation powers. These observations can be qualitatively understood from polymorphic heterostructures between wurtzite silicon and cubic silicon induced by stacking faults in silicon nanowires.

Silicon nanowires were synthesized *via* chemical vapor deposition (CVD) at 550 °C in a tube furnace. Au nanoparticles were used as catalysts and SiH_4 (100 sccm, 2% diluted in H_2) was used as the silicon source. A growth pressure of ~100 Torr was maintained by mechanically adjusting the pumping speed through a vacuum valve. Fig. 1 shows scanning electron microscopy (SEM) pictures of silicon nanowires. Unlike typical CVD nanowires, these nanowires have a chain-like structure due to periodic instability.[14,15] Cross-sectional transmission electron microscopy (TEM) micrographs in Fig. 2 indicate that nanowires contain a high density of stacking faults. High resolution TEM and electron diffraction (through fast Fourier transform (FFT)) reveal the existence of twinning and high density stacking fault (SF) areas. Based on the FFT diffraction patterns (Fig. 2c and 2d), area b-1 is a typical cubic structure across a twin interface with very strong (111) diffraction dots (marked in Fig. 2c). Instead, area b-2 has a distinctive rectangular diffraction pattern with stronger diffractions indexed as (0002) and $(11\bar{2}2)$, as marked in Fig. 2d. These diffraction features suggest a local wurtzite structure caused by the high stacking faults in the area.[16] The chain-like morphology and high density stacking faults are induced mainly by the relatively high growth temperature and pressure.[17]

Photoluminescence measurements were performed at room temperature using a backscattering configuration with a 532 nm laser as an excitation source. The emitted light was collected and analyzed by a single-grating spectrometer

[a]*Department of Electrical and Computer Engineering, University of Houston, Houston, TX 77204, USA. E-mail: jbao@uh.edu*
[b]*Ingram School of Engineering, and Materials Science, Engineering and Commercialization Program, Texas State University, San Marcos, TX 78666, USA. E-mail: qy10@txstate.edu*
[c]*Department of Chemistry, Boston College, Chestnut Hill, MA 02467, USA*
[d]*Department of Electrical and Computer Engineering, Texas A&M University, College Station, Texas 77843, USA*
† Electronic supplementary information (ESI) available. See DOI: 10.1039/c4nr05410e

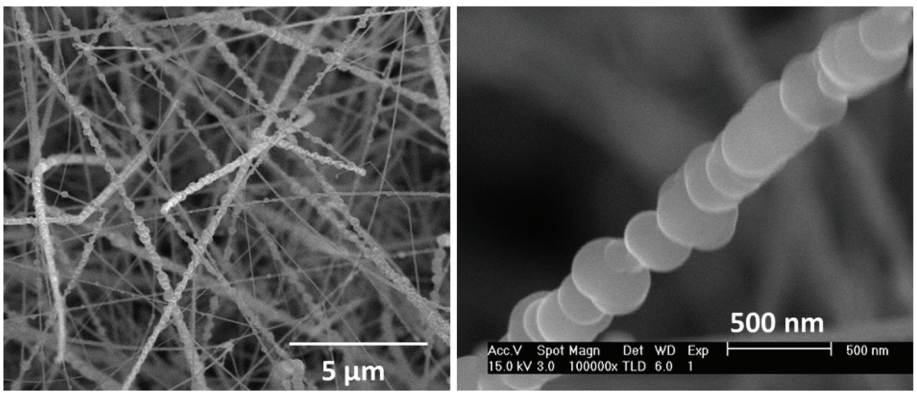

Fig. 1 Scanning electron microscopy (SEM) images of Si nanowires synthesized using chemical vapor deposition (CVD).

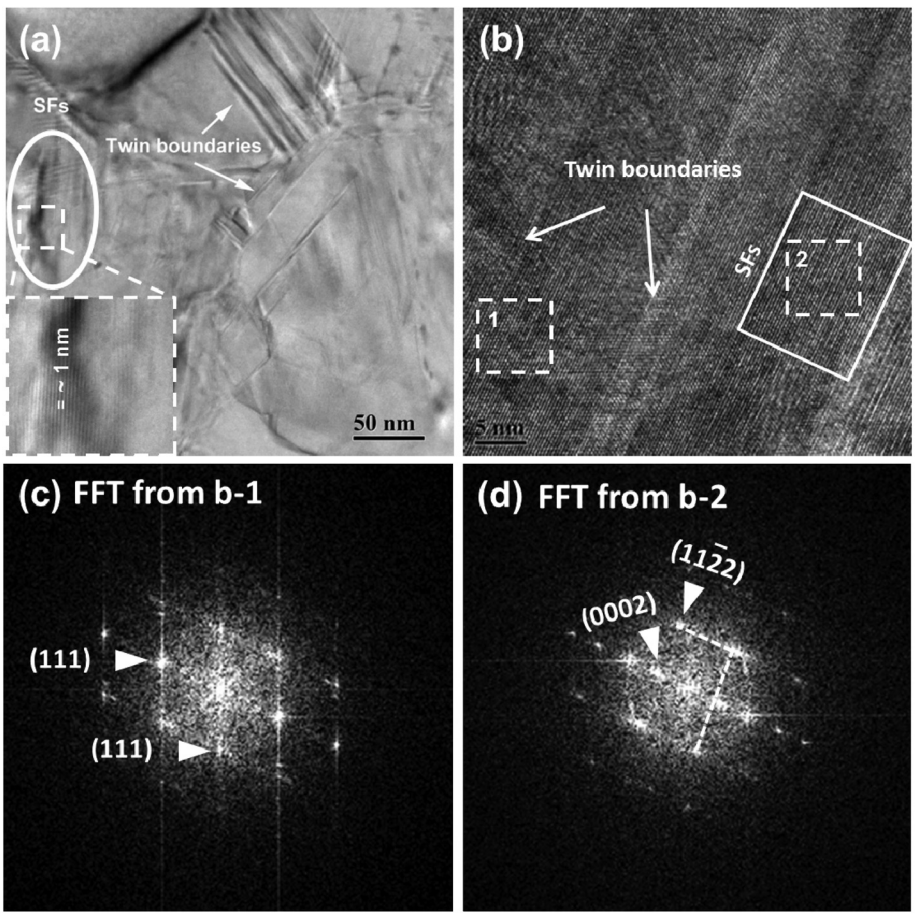

Fig. 2 Cross-sectional TEM study of Si nanowires: (a) high-density stacking faults in low magnification, (b) twin boundaries in high resolution TEM with obvious stacking fault areas marked; (c, d) fast Fourier transforms (FFTs) of areas b-1 and b-2 showing cubic and wurtzite diffractions, respectively.

(Horiba iHR320) equipped with two separate detectors: a silicon charge coupled device (CCD) for the visible spectrum, and an InGaAs array detector for infrared light from 1000 to 1600 nm. The same experimental configuration was used for all the samples presented in this work.

Photoluminescence was first studied in the visible spectrum. As can be seen in Fig. 3a, the nanowires exhibit a broad emission centered at 650 nm. The integrated intensity increases with incident light at low powers, but the intensity starts to saturate at 110 mW. Further increase in incident power only makes the peak luminescence weaker, but the emission at longer wavelength begins to appear. The infrared emission is confirmed in Fig. 3b using the InGaAs detector, it is a broad spectrum extended to 1.6 μm. Different from visible

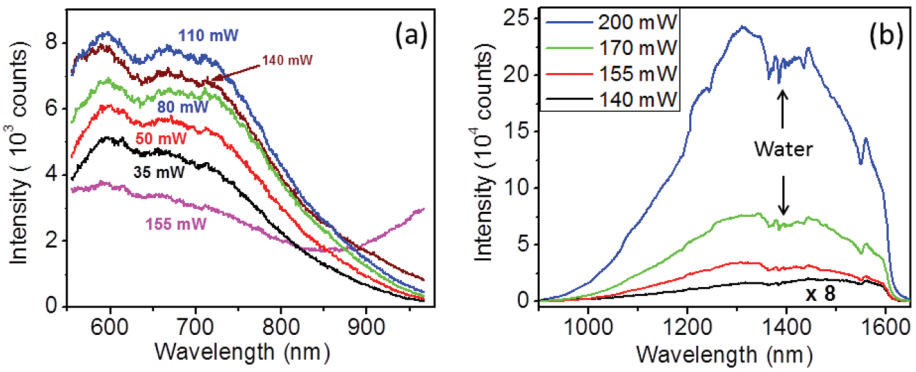

Fig. 3 (a) Visible and (b) infrared photoluminescence spectra of CVD silicon nanowires at several different excitation powers. The infrared spectrum at 140 mW is enlarged by 8. The absorption near 1.4 μm is due to water in air.

spectra, the integrated intensity increases super-linearly with increase in the incident power. The infrared emission below 140 mW was too weak to be measured; it also became weaker and broader, and showed slight redshift when the incident power exceeded 200 mW.

Sub-bandgap infrared emissions have been observed in different silicon nanostructures. Jia *et al.* reported infrared cathode luminescence in silicon nanowires synthesized using thermal evaporation of SiO.[12] They attributed the emission to dislocations because of the distinctive spectral features. The same group also reported broad-band infrared photoluminescence peaked at 1.5 μm in porous silicon, and they ascribed the emission to Si/SiO_2 interfaces.[11] As shown in Fig. 3b, our infrared emission spectra are centered at 1350 nm, and are different from those reported. Infrared photoluminescence was also observed in silicon nanocrystal thin films, but the origin of the emission was not clearly identified.[13] It should be noted that the contribution of blackbody radiation to the infrared emission due to laser heating can be totally neglected in our case. Based on the position of silicon optical phonon, we estimated that the temperature of nanowires increased to less than 200 °C under the strongest excitation at 200 mW. We believe this increase in temperature was responsible for the quenching of visible emission at a higher incident power shown in Fig. 3a.

In order to identify the origin of both visible and infrared emissions in CVD silicon nanowires, we measured photoluminescence in defect-free silicon nanocrystals (SiNCs) and etched silicon nanowires.[4,18,19] Both nanostructures contain considerable amount of Si/SiO_2 interfaces as CVD nanowires. Fig. 4 shows photoluminescence spectra of electroless etched silicon nanowires (EE SiNWs).[19] A similar broad band visible emission can be found, but no infrared emission can be detected. The nanowires have an average diameter of 170 nm. Since these EE SiNWs were obtained from p-type high quality silicon wafers, they are almost free of any defects such as stacking faults.[18] Fig. 5 shows photoluminescence spectra of silicon nanocrystals embedded in an oxide matrix.[4] Very strong photoluminescence can be seen in the visible and near infrared regions above the band gap. Again, like EE SiNWs, infrared emission below the band gap was not detected in a similar range of excitation powers. The shift in the peak position is due to the change in the size of nanocrystals.

The above control experiments have helped us to understand the origins of luminescence in different silicon nanostructures. Let us first look at the visible spectra. The size-dependent visible emission in SiNCs is clearly a result of quantum confinement, and the broad visible emission in CVD NWs and EE NWs come from the Si/SiO_2 interface. Both types of nanowires are too big to exhibit any quantum confinement

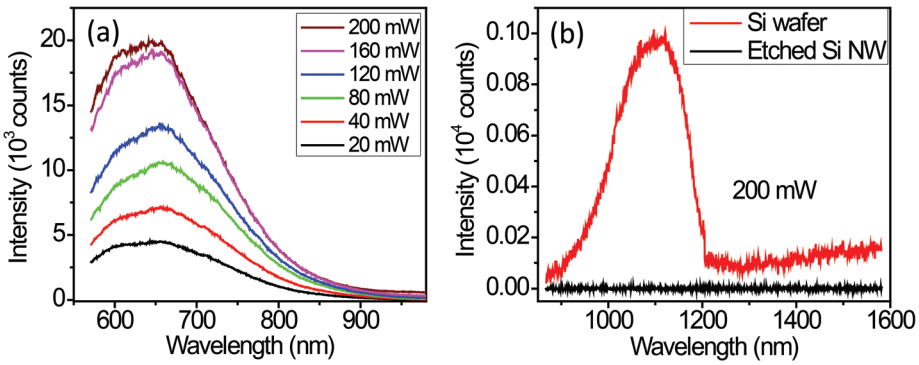

Fig. 4 (a) Visible and (b) infrared photoluminescence spectra of electroless etched silicon nanowires. No infrared emission is detected. As comparison, band gap photoluminescence at 1100 nm can be observed in a silicon substrate.

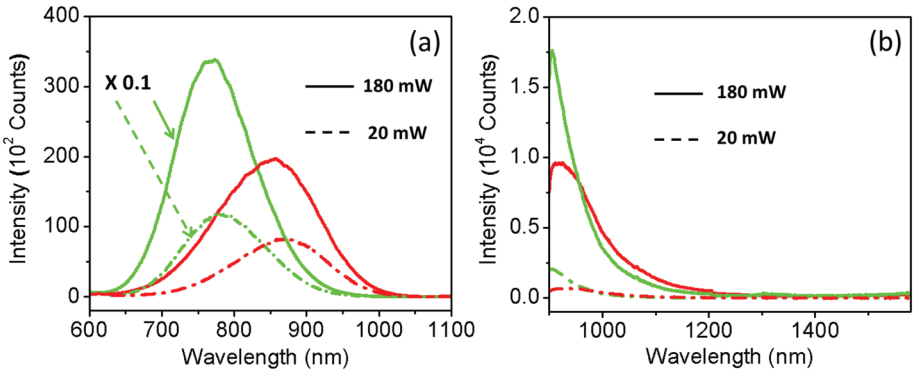

Fig. 5 (a) Visible and (b) infrared photoluminescence spectra of silicon nanocrystals with large (in red) and smaller (in green) sizes under excitations of two representative laser powers: 20 mW (dashed lines) and 180 mW (solid lines).

effect, and photoluminescence from Si/SiO_2 interfaces in the silicon NC/SiO_2 matrix is too weak to be observed due to the much stronger size-dependent emission from silicon nanocrystals. Compared with photoluminescence of an ordinary silicon substrate shown in Fig. 4b, neither CVD nor EE nanowires exhibit band-gap photoluminescence at 1.1 μm, apparently due to a large surface recombination velocity associated with the large surface to volume ratio of nanowires. The reason why visible photoluminescence in EE SiNWs did not suffer from thermal quenching was because EE SiNWs were in intimate contact with the silicon substrate so that laser heating was not as significant as in CVD nanowires.

Based on the above observation that no infrared emission was detected in both EE SiNWs and SiNCs, we can conclude that the broad band infrared emission must be related to the unique stacking fault crystal structures in CVD SiNWs. Stacking faults, especially twinning, can create a mixed structure of wurtzite and cubic silicon lattices. The effect of twinning on the optical properties was first reported by one of the authors.[20] The same mechanism can qualitatively explain main features of the observed infrared photoluminescence spectra in CVD silicon nanowires. A twinned nanowire is different from a defect-free nanowire because a twin plane has wurtzite symmetry locally: it is one unit of wurtzite crystal that is different from the neighboring cubic or diamond structure.[21–24] Thicker wurtzite crystals can be created by consecutive twinning. Previous calculations and photoconductivity measurements indicated that wurtzite silicon is an indirect semiconductor with a bandgap of ~0.8 eV.[25–30] It was also confirmed by recent cathodoluminescence study of wurtzite silicon nanowires at room temperature.[31] Because wurtzite silicon and conventional cubic silicon form a type-I band alignment,[30] a randomly twinned silicon nanowire can be regarded as a mixture of wurtzite/cubic quantum wells with a random distribution of well thickness.

The effect of wurtzite/cubic quantum well heterostructure on the optical properties is two-fold. First, quantum confinement can create localization of photoexcited carriers, thus enhancing the radiative recombination. Because of the nature of the indirect band gap of wurtzite silicon, such enhancement is important for strong light emission. Second, depending on the thickness of wurtzite/cubic quantum well, the emission wavelength can be varied in a wide range between wurtzite and cubic bandgaps. We believe that the broad infrared emission is due to the random distribution of wurtzite/cubic quantum well thickness.[20] The blue-shift of the peak position under higher excitation powers is due to the band filling effect.[20] Because of high density of non-radiative channels associated with the large surface to volume ratio as well as a large number of structural defects, infrared emission was only observed at a relatively large excitation power, resulting in a super-linear increase of infrared emission intensity.

Twinning is the simplest form of stacking faults. Although it can alter the crystal structures, it will not create non-radiative defects because it does not change the local bonding between silicon atoms. Due to the unstable growth conditions, we believe that many stacking faults are not simple twinning, and they will induce many non-radiative defect centers, which make the infrared emission very weak under low excitation powers.

Wurtzite Si (Si IV) was initially created using high-temperature indentation of diamond (cubic) Si,[25,32] it was later prepared by pulsed laser-beam annealing or laser ablation.[33,34] The wurtzite Si structure was also identified in CVD Si nanowires.[16,35,36] Recently, uniform wurtzite silicon shells were epitaxially grown on hexagonal GaP nanowire cores.[37] Despite these developments in the synthesis of wurtzite silicon, a bandgap confirmation using photoluminescence has not been reported.

Conclusions

In conclusion, we have observed room-temperature broadband sub-bandgap photoluminescence in stacking faulted silicon nanowires. The infrared emission comes from wurtzite/cubic silicon heterostructures. A narrow band infrared emission can in principle be obtained by creating a pure structure of the wurtzite silicon lattice. Because wurtzite silicon is intimately integrated with conventional cubic silicon, nanowires

with embedded wurtzite structures can be used to make sub-bandgap infrared light sources or photodetectors for integrated silicon photonic circuits.

Acknowledgements

J.B. and Q.Y acknowledge the support from the National Science Foundation (DMR-0907336 monitored by Charles Ying; Career Award ECCS-1240510 monitored by Anupama Kaul) and the Robert A Welch Foundation (E-1728). The TEM work at Texas A&M University was funded by the U.S. National Science Foundation (DMR-0846504).

Notes and references

1 L. P. S. Ossicini, F. Priolo and S. Ossicini, *Light Emitting Silicon for Microphotonics*, Springer-Verlag, Berlin, 2003.
2 L. T. Canham, *Appl. Phys. Lett.*, 1990, **57**, 1046–1048.
3 L. Pavesi, L. Dal Negro, C. Mazzoleni, G. Franzo and F. Priolo, *Nature*, 2000, **408**, 440–444.
4 Z. H. Liu, J. D. Huang, P. C. Joshi, A. T. Voutsas, J. Hartzell, F. Capasso and J. M. Bao, *Appl. Phys. Lett.*, 2010, **97**, 071112.
5 G. Davies, *Phys. Rep.*, 1989, **176**, 83–188.
6 B. Zheng, J. Michel, F. Y. G. Ren, L. C. Kimerling, D. C. Jacobson and J. M. Poate, *Appl. Phys. Lett.*, 1994, **64**, 2842–2844.
7 S. G. Cloutier, P. A. Kossyrev and J. Xu, *Nat. Mater.*, 2005, **4**, 887–891.
8 V. Kveder, M. Badylevich, E. Steinman, A. Izotov, M. Seibt and W. Schroter, *Appl. Phys. Lett.*, 2004, **84**, 2106–2108.
9 J. M. Bao, M. Tabbal, T. Kim, S. Charnvanichborikarn, J. S. Williams, M. J. Aziz and F. Capasso, *Opt. Express*, 2007, **15**, 6727–6733.
10 Y. Yang, J. M. Bao, C. Wang and M. J. Aziz, *J. Appl. Phys.*, 2010, **107**, 123109.
11 G. B. Jia, W. Seifert, T. Arguirov and M. Kittler, *J. Mater. Sci.:Mater. Electron.*, 2008, **19**, S9–S13.
12 G. Jia, T. Arguirov, M. Kittler, Z. Su, D. Yang and J. Sha, *Semiconductors*, 2007, **41**, 391–394.
13 S. Binetti, M. Acciarri, M. Bollani, L. Fumagalli, H. von Kanel and S. Pizzini, *Thin Solid Films*, 2005, **487**, 19–25.
14 E. I. Givargizov, *J. Cryst. Growth*, 1973, **20**, 217–226.
15 H. Kohno and S. Takeda, *J. Cryst. Growth*, 2000, **216**, 185–191.
16 J. Arbiol, B. Kalache, P. R. I. Cabarrocas, J. R. Morante and A. F. I. Morral, *Nanotechnology*, 2007, **18**, 8.
17 X. H. Liu and D. W. Wang, *Nano Res.*, 2009, **2**, 575–582.
18 R. Liu, C. Stephani, J. J. Han, K. L. Tan and D. W. Wang, *Angew. Chem., Int. Ed.*, 2013, **52**, 4225–4228.
19 G. B. Yuan, K. Aruda, S. Zhou, A. Levine, J. Xie and D. W. Wang, *Angew. Chem., Int. Ed.*, 2011, **50**, 2334–2338.
20 J. M. Bao, D. C. Bell, F. Capasso, J. B. Wagner, T. Martensson, J. Tragardh and L. Samuelson, *Nano Lett.*, 2008, **8**, 836–841.
21 Z. Z. Bandic and Z. Ikonic, *Phys. Rev. B: Condens. Matter*, 1995, **51**, 9806–9812.
22 K. Hiruma, M. Yazawa, T. Katsuyama, K. Ogawa, K. Haraguchi, M. Koguchi and H. Kakibayashi, *J. Appl. Phys.*, 1995, **77**, 447–462.
23 J. E. Northrup and M. L. Cohen, *Phys. Rev. B: Condens. Matter*, 1981, **23**, 2563–2566.
24 C. Y. Yeh, Z. W. Lu, S. Froyen and A. Zunger, *Phys. Rev. B: Condens. Matter*, 1992, **46**, 10086–10097.
25 J. M. Besson, E. H. Mokhtari, J. Gonzalez and G. Weill, *Phys. Rev. Lett.*, 1987, **59**, 473–476.
26 J. Joannopoulos and M. L. Cohen, *Phys. Rev. B: Solid State*, 1973, **7**, 2644–2657.
27 C. Raffy, J. Furthmuller and F. Bechstedt, *Phys. Rev. B: Condens. Matter*, 2002, **66**, 075201.
28 M. T. Yin and M. L. Cohen, *Phys. Rev. B: Condens. Matter*, 1982, **26**, 5668–5687.
29 B. D. Malone, J. D. Sau and M. L. Cohen, *Phys. Rev. B: Condens. Matter*, 2008, **78**, 035210.
30 M. Murayama and T. Nakayama, *Phys. Rev. B: Condens. Matter*, 1994, **49**, 4710–4724.
31 F. Fabbri, E. Rotunno, L. Lazzarini, N. Fukata and G. Salviati, *Sci. Rep.*, 2014, **4**, 3603.
32 R. H. Wentorf and J. S. Kasper, *Science*, 1963, **139**, 338.
33 J. H. Kim and J. Y. Lee, *Mater. Lett.*, 1996, **27**, 275–279.
34 Y. Zhang, Z. Iqbal, S. Vijayalakshmi and H. Grebel, *Appl. Phys. Lett.*, 1999, **75**, 2758–2760.
35 A. F. I. Morral, J. Arbiol, J. D. Prades, A. Cirera and J. R. Morante, *Adv. Mater.*, 2007, **19**, 1347–1351.
36 F. J. Lopez, U. Givan, J. G. Connell and L. J. Lauhon, *ACS Nano*, 2011, **5**, 8958–8966.
37 R. E. Algra, M. Hocevar, M. A. Verheijen, I. Zardo, G. G. W. Immink, W. J. P. van Enckevort, G. Abstreiter, L. P. Kouwenhoven, E. Vlieg and E. Bakkers, *Nano Lett.*, 2011, **11**, 1690–1694.